Chromobox Protein Homologue 7 Protein, with Decreased Expression in Human Carcinomas, Positively Regulates E-Cadherin Expression by Interacting with the Histone Deacetylase 2 Protein

Antonella Federico,[1,3] Pierlorenzo Pallante,[1,3] Mimma Bianco,[1] Angelo Ferraro,[3] Francesco Esposito,[1] Maria Monti,[4] Marianna Cozzolino,[4] Simona Keller,[1,3] Monica Fedele,[1] Vincenza Leone,[1,3] Giancarlo Troncone,[2,3] Lorenzo Chiariotti,[1,3] Piero Pucci,[4] and Alfredo Fusco[1,3]

[1]Istituto di Endocrinologia ed Oncologia Sperimentale del CNR c/o Dipartimento di Biologia e Patologia Cellulare e Molecolare and [2]Dipartimento di Anatomia Patologica e Citopatologia, Facoltà di Medicina e Chirurgia di Napoli, Università degli studi di Napoli "Federico II"; [3]Naples Oncogenomic Center-CEINGE, Biotecnologie Avanzate-Napoli, and European School of Molecular Medicine-Naples Site; [4]CEINGE, Biotecnologie Avanzate-Napoli e Dipartimento di Chimica Organica e Biochimica, Università degli studi di Napoli "Federico II," Naples, Italy

Abstract

Chromobox protein homologue 7 (CBX7) is a chromobox family protein encoding a novel polycomb protein, the expression of which shows a progressive reduction, well related with the malignant grade of the thyroid neoplasias. Indeed, CBX7 protein levels decreased in an increasing percentage of cases going from benign adenomas to papillary, follicular, and anaplastic thyroid carcinomas. To elucidate the function of CBX7 in carcinogenesis, we searched for CBX7 interacting proteins by a proteomic analysis. By this approach, we identified several proteins. Among these proteins, we selected histone deacetylase 2 (HDAC2), which is well known to play a key role in neoplastic cell transformation and down-regulation of E-cadherin expression, the loss of which is a critical event in the epithelial-to-mesenchymal transition. We confirmed by coimmunoprecipitation that CBX7 physically interacts with the HDAC2 protein and is able to inhibit its activity. Then, we showed that both these proteins bind the *E-cadherin* promoter and that CBX7 up-regulates E-cadherin expression. Consistent with these data, we found a positive statistical correlation between CBX7 and E-cadherin expression in human thyroid carcinomas. Finally, we showed that the expression of CBX7 increases the acetylation status of the histones H3 and H4 on the *E-cadherin* promoter. Therefore, the ability of CBX7 to positively regulate E-cadherin expression by interacting with HDAC2 and inhibiting its activity on the *E-cadherin* promoter would account for the correlation between the loss of CBX7 expression and a highly malignant phenotype. [Cancer Res 2009;69(17):7079–87]

Introduction

Chromobox protein homologue 7 (*CBX7*) gene encodes a novel polycomb protein of 28.4 kDa and 251 amino acids, which contains a "chromodomain" between amino acids 10 and 46 (1, 2). CBX7 is a chromobox family protein and a member of the polycomb

repressive complex 1, which, together with the polycomb repressive complex 2, maintains developmental regulatory genes in a silenced state (3–5). Mouse Cbx7 associates with facultative heterochromatin and with the inactive X chromosome, suggesting a role of the Cbx7 protein in the repression of gene transcription (6, 7). We have found previously that the *CBX7* gene was drastically down-regulated in six thyroid carcinoma cell lines versus normal thyroid cells. Subsequently, the analysis of CBX7 expression in a large number of thyroid carcinoma samples revealed a progressive reduction of CBX7 levels that was well related with the malignant grade of the thyroid neoplasias (8). Indeed, it decreased in an increasing percentage of cases going from benign adenomas to papillary, follicular, and anaplastic thyroid carcinomas (9, 10). The analysis of rat and mouse models of thyroid carcinogenesis gave rise to very similar results (8). More recent results confirmed a correlation between low CBX7 expression and a reduced survival in colon carcinoma patients.[5] Moreover, the association between lack of CBX7 expression and a more aggressive histotype has also been shown by our group in breast, ovary, and prostate carcinomas.[6] Restoration of CBX7 expression in thyroid cancer cells reduced their growth rate, indicating that CBX7 plays a critical role in the regulation of transformed thyroid cell proliferation (8).

The aim of the present work has been to elucidate the mechanisms by which the loss of CBX7 is involved in carcinogenesis, attempting to identify the CBX7 protein partners by performing a functional proteomic experiment. Here, we show that CBX7 interacts with histone deacetylase 2 (HDAC2) and inhibits its activity. Moreover, both HDAC2 and CBX7 bind the *E-cadherin* (*CDH1*) promoter, and CBX7 contrasts the inhibiting effect of HDAC2 on E-cadherin expression.

Therefore, the ability of CBX7 to positively regulate E-cadherin expression might account for the correlation of the loss of CBX7 expression with a highly malignant phenotype in cancer patients.

Materials and Methods

Cell culture and transfections. TPC1 and NPA (derived from thyroid papillary carcinomas) and PC Cl3, HEK 293, and HeLa cells were grown as described previously (8, 11). PC Cl3 cells are differentiated thyroid cells of 18-month-old rat Fischer origin depending on thyrotropine for the growth (12). For the inhibition of CBX7 expression, rat *Cbx7* small interfering RNA

---

[5] Pallante et al., submitted for publication.
[6] Pallante, Terracciano, and Troncone, manuscript in preparation.
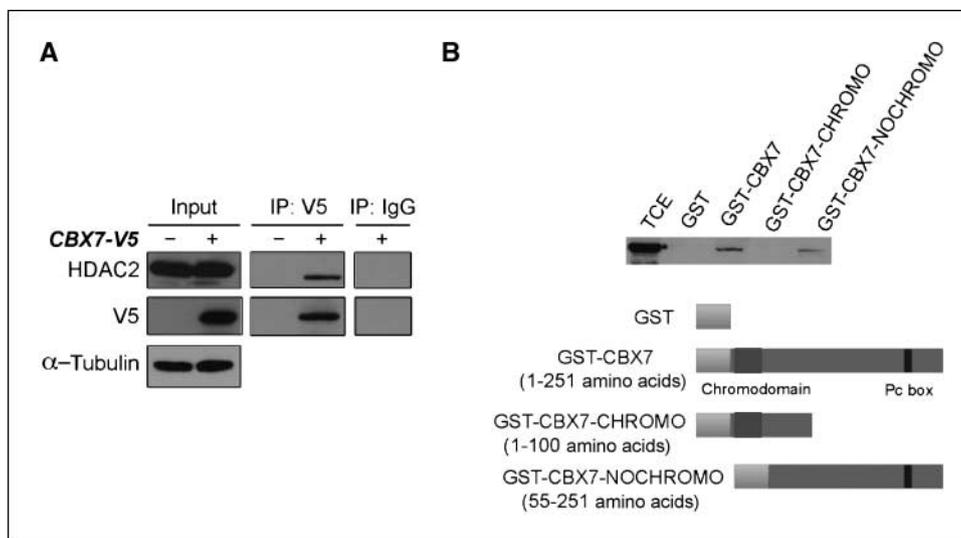
Cancer Research

Figure 1. CBX7 interacts with HDAC2. *A,* HEK 293 cells were transiently transfected with V5-tagged CBX7 or empty vector and total cell extracts (*TCE*) were coimmunoprecipitated using anti-V5 antibodies. Immunocomplexes were analyzed by Western blot with either anti-V5 or anti-HDAC2 antibodies. IgG indicates the negative control of immunoprecipitation using an unrelated antibody. *B,* GST pull-down assay with GST or recombinant GST-CBX7 proteins (wild-type and mutants as schematically reported below). The filter was incubated with an anti-HDAC2 antibody.

(SI01495795 and SI01495802; Qiagen) and nonsilencing control small interfering RNA (1022076; Qiagen) were transfected using Oligofectamine (Invitrogen) according to the manufacturer's recommendations. *CBX7*-inducible NPA cells were generated by transfecting NPA cells with the pcDNA6/TR regulatory vector (Invitrogen). Trichostatin A (Sigma) treatments were done for 24 h after transfection.

Plasmids. V5-tagged CBX7 expression plasmid was generated by the insertion of the PCR product *CBX7* cDNA into pcDNA-DEST-40 Gateway Vector (Invitrogen). HA-tagged CBX7 expression plasmid was obtained by PCR amplification and subcloned into the pCefl-HA expression vector. CBX7-deletion mutants were cloned in pCefl-HA as well.

Protein extraction, Western blotting, and immunoprecipitation assays. Protein extraction, Western blotting, and coimmunoprecipitation procedures were carried out as reported elsewhere (13). The antibodies used for immunoprecipitation and Western blotting were anti-CBX7 (8), anti-HA (Roche), anti-V5 (Sigma), anti-pan-cadherin (Sigma), and anti-α-tubulin (Sigma).

GST pull-down experiments. GST fusion proteins were constructed by cloning the human cDNA sequence in a pGEX4T-1 vector (Promega). GST pull-down experiments were carried out as reported elsewhere (14).

HDAC activity assay. Cells were transfected with increasing amount of CBX7 expression vector and were used to assay the HDAC activity according to the manufacturer's instructions of Histone Deacetylase Assay Kit (Upstate).

Fresh human thyroid tissue samples. Neoplastic human thyroid tissues and normal adjacent tissue or the normal contralateral thyroid lobe were obtained as described previously (8).

RNA extraction, reverse transcription, and PCR analysis. Total RNA isolation and reverse transcription-PCR (RT-PCR) from human tissues were done as described previously (8, 15). Each reaction was carried out in duplicate. We used the $2^{-\Delta\Delta CT}$ method to calculate relative expression levels (16, 17). Detailed primer sequences are available as Supplementary Materials and Methods.

Immunohistochemistry. Immunohistochemical analysis were done as described previously (8).

Electrophoretic mobility shift assay. For gel shift analysis, nuclear extracts were prepared as described elsewhere (18) and electrophoretic mobility shift assay was done as described previously (19). The double-strand oligonucleotides covered a region spanning from nucleotide −70 to +54 of the human *E-cadherin* promoter with respect to the transcription start site (TSS).

Chromatin immunoprecipitation and re-chromatin immunoprecipitation assays. After transfection, chromatin samples were processed for chromatin immunoprecipitation and re-chromatin immunoprecipitation experiments as reported elsewhere (19). Samples were subjected to immunoprecipitation with the following specific antibodies: anti-HA

(Roche) and anti-HDAC2, anti-H3K4m2, anti-H3K4m3, anti-H3K9me, anti-H3K9m3, and anti-H4K20 (Upstate). The sequences of the used primers are available as Supplementary Materials and Methods.

Transactivation assay. Cells were transiently transfected with the reporter construct in which the luciferase gene was driven by described fragments of *E-cadherin* promoter (20, 21) and normalized with the use of a cotransfected β-galactosidase construct. Luciferase activity was analyzed by Dual-Light System (Applied Biosystems).

DNA extraction and methylation analysis. DNA was prepared using QIAamp DNA Mini Kit (Qiagen) following the instruction manual. PCR primers to analyze *E-cadherin* promoter were designed by using Methprimer (22). The MassCLEAVE biochemistry was done as described previously (23). Mass spectra were acquired by using a MassARRAY Compact matrix-assisted laser desorption/ionization—time-of-flight (Sequenom) and spectra methylation ratios were generated by the Epityper software version 1.0 (Sequenom).

Statistical analysis. For the comparison between two groups of experiments, Student's *t* test was used. The statistical significant difference was considered when $P < 0.05$. A Pearson correlation coefficient (R^2) close to 1 was considered indicative of a significant direct correlation. All experiments were done in triplicate and the data are mean ± SD of three independent experiments.

Results

CBX7 physically interacts with HDAC2 protein. To investigate the mechanisms by which the loss of CBX7 expression correlates with the highly malignant phenotype, we searched for CBX7 interacting proteins by performing a functional proteomic analysis. Therefore, we transiently transfected the HEK 293 cells with a V5-tagged CBX7 expression vector, immunoprecipitated the nuclear protein lysates with anti-V5 antibodies (Supplementary Fig. S1*A*), and fractionated the immunoprecipitated material on a 12% one-dimensional gel and stained with colloidal Coomassie (Supplementary Fig. S1*B*). After SDS-PAGE, single components of the immunoprecipitated complexes were analyzed by mass spectrometry (24). In Supplementary Table S1, we report some representative CBX7 interacting proteins. Among them, we focused our attention on HDAC2 because of its relevance in tumor biology (25). HDACs catalyze the removal of acetyl groups from core histones and, because of their ability to induce local condensation of chromatin, are generally considered repressors of transcription.

To verify the CBX7/HDAC2 interaction *in vivo*, HEK 293 cells were transiently transfected with the V5-tagged CBX7 expression

vector. Protein lysates were immunoprecipitated with either anti-V5 or anti-HDAC2 antibodies and immunoblotted with both anti-V5 and anti-HDAC2 antibodies (Fig. 1A; Supplementary Fig. S1C). As shown in Fig. 1A, we detected the association between CBX7 and the endogenous HDAC2 protein, confirming that CBX7 and HDAC2 form complexes *in vivo*.

To further examine the specificity of this interaction, and to map the regions of CBX7 protein required for the binding to HDAC2, pull-down assays were done incubating total cell extracts deriving from HEK 293 cells, with the CBX7 recombinant protein fused to GST (GST-CBX7) and with two deletion mutants of CBX7: GST-CBX7-CHROMO (1-100 amino acids) and GST-CBX7-NOCHROMO (55-251 amino acids). As shown in Fig. 1B, HDAC2 interacts with both GST-CBX7 and GST-CBX7-NOCHROMO mutants but not with the GST alone or the GST-CBX7-CHROMO mutant. These results clearly show that the CBX7 chromodomain is not required for the interaction between CBX7 and HDCA2.

CBX7 inhibits HDAC activity. To evaluate the effects of the CBX7/HDAC2 interaction on the HDAC2 activity, nuclear extracts from HeLa and NPA cells were prepared and the ability of increasing amount of transfected *CBX7* to modulate HDAC activity was tested using a HDAC activity assay. CBX7 expression significantly inhibited HDAC activity in a dose-dependent manner (the percentage of inhibition was 65.15% and 42.55% in HeLa and NPA cells, respectively, after the transfection of 10 μg *CBX7* expression vector; Fig. 2A and B). As positive control for HDAC inhibition, we used 250 mmol/L sodium butyrate, a strong HDAC inhibitory compound (26, 27). Nuclear extracts from NPA transfected with *CBX7* were immunoprecipitated with anti-HDAC2 antibodies. Then, immunoprecipitated material was tested using a HDAC activity assay. As shown in Fig. 2C, CBX7 specifically inhibited HDAC2 activity.

CBX7 binds to the *E-cadherin* gene promoter. It has been recently shown that HDAC2 is involved in the repressive complex that silences the *E-cadherin* gene expression during tumor progression (28). E-cadherin is emerging as one of the caretakers of the epithelial phenotype because the loss of its expression has been shown to be a critical event of epithelial-to-mesenchymal transition (29, 30). Therefore, to evaluate whether CBX7 was able to bind the *E-cadherin* promoter *in vitro*, we performed an electrophoretic mobility shift assay. Nuclear extracts from HEK 293

cells transiently transfected with either V5-tagged CBX7 or empty vectors were incubated with a radiolabeled oligonucleotide corresponding to the *E-cadherin* promoter. As shown in Fig. 3A, the *E-cadherin* oligonucleotide forms a specific complex (indicated in the figure as A) with nuclear proteins of cells transfected with V5-tagged CBX7, which was not present in mock-transfected cells (compare *lanes 1* and *2*). Binding specificity was shown by incubating the nuclear extract with a 100-fold molar excess of unlabeled *E-cadherin* oligonucleotide (*lanes 3* and *4*).

Then, HEK 293 and HeLa cells were transiently transfected with HA-tagged CBX7 expression vector, tested by Western blotting for protein expression (Fig. 3B), crosslinked, and immunoprecipitated with anti-HA or IgG antibodies. Immunoprecipitation of chromatin was subsequently analyzed by semiquantitative PCR using primers spanning the region of the *E-cadherin* promoter (−300 bp upstream to +40 bp downstream to the TSS). Anti-HA antibodies precipitated this *E-cadherin* promoter region from HEK 293 and HeLa cells transfected with HA-tagged CBX7 protein. No immunoprecipitation was observed with IgG precipitates, and when primers for the control promoter *GAPDH* were used (Fig. 3B), indicating that the binding is specific for the *E-cadherin* promoter. Similar results were obtained when NPA cells were used (data not shown). These results indicate that CBX7 binds the *E-cadherin* promoter region *in vivo*.

Then, to investigate whether the physical interaction between CBX7 and HDAC2 takes place on the human *E-cadherin* promoter, we performed re-chromatin immunoprecipitation analysis. HEK 293 cells transiently transfected with HA-tagged CBX7 were crosslinked and immunoprecipitated with anti-HDCA2 antibodies. The anti-HDAC2 complexes were released, re-immunoprecipitated with anti-HA antibodies, and then analyzed by PCR. The results shown in Fig. 3C reveal that the antibodies against HA precipitate the *E-cadherin* promoter after their release from anti-HDAC2, indicating that CBX7 occupies this promoter region together with HDAC2. The reciprocal experiment provided comparable results (Fig. 3D). Taken together, these results indicate that CBX7 binds the human *E-cadherin* promoter *in vivo* and participates in the same DNA-bound complexes that contain HDAC2.

CBX7 positively regulates the *E-cadherin* promoter. To evaluate the effect of CBX7 expression on *E-cadherin* transcription, HEK 293 cells were transiently cotransfected with an expression
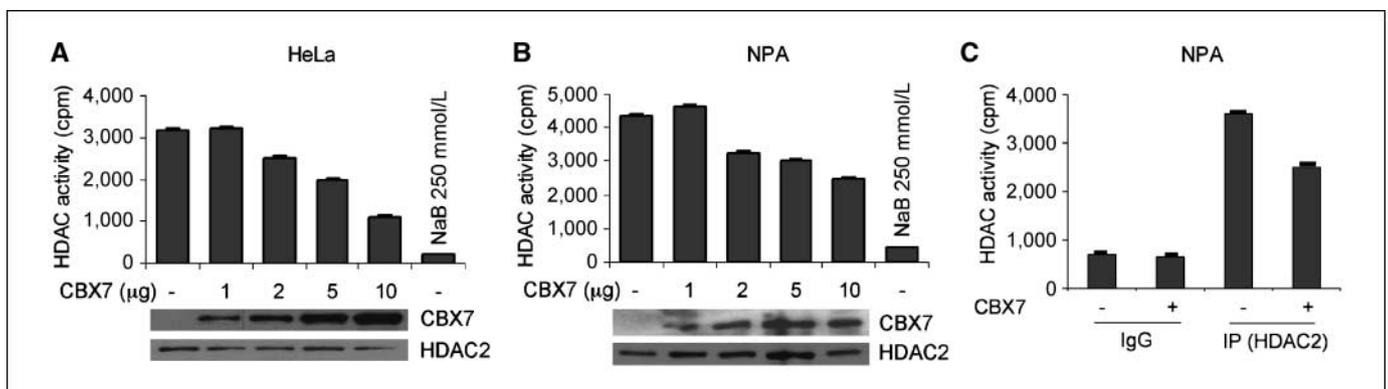

Figure 2. CBX7 inhibits HDAC activity. HeLa and NPA cells (*A* and *B*, respectively), transiently transfected with increasing amounts of CBX7 expression vector, were assayed for HDAC activity. Samples treated with sodium butyrate (*NaB*) were used as positive control of HDAC activity inhibition. Aliquots of the same lysates were immunoblotted with the indicated antibodies (*bottom*). *C*, NPA cells were transiently transfected with the CBX7 expression vector or the empty vector. Nuclear extracts were immunoprecipitated using anti-HDAC2 antibodies and assayed for HDAC activity. Mean ± SD of three independent experiments.
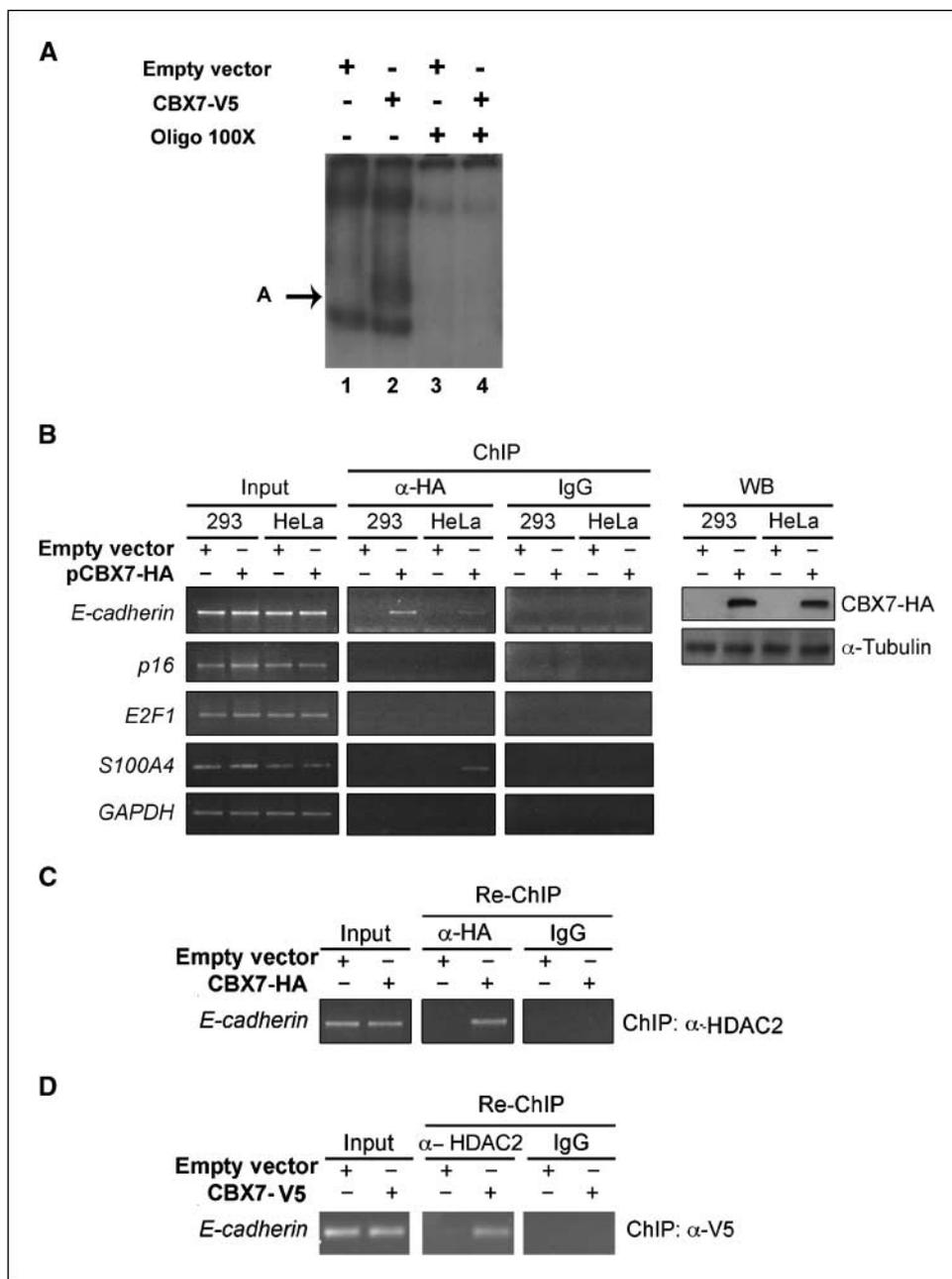
Figure 3. CBX7 binds to the *E-cadherin* gene promoter. *A,* electrophoretic mobility shift assay with nuclear extracts from HEK 293 cells transiently transfected with the V5-tagged CBX7 expression vector or the empty vector using the oligonucleotide spanning from nucleotide −70 to +54 of the human *E-cadherin* promoter as a probe. To assess the specificity of the binding, nuclear extracts were incubated in the presence of a 100-fold excess of unlabeled oligonucleotide used as competitor. *B,* chromatin immunoprecipitation (*ChIP*) assay using anti-HA antibodies in HEK 293 and HeLa cells transiently transfected with HA-tagged CBX7 or the empty vector. The associated DNA was amplified by PCR using primers specific for the human gene promoters (*left*). For the *E-cadherin* promoter, a region spanning from nucleotide −300 to +40 of the gene with respect to the TSS was used. IgGs were used as an immunoprecipitation control. *C,* re-chromatin immunoprecipitation experiments in which soluble chromatin immunoprecipitated with anti-HDAC2 was re-immunoprecipitated with anti-HA. IgG control refers to re-chromatin immunoprecipitation with anti-HA. *D,* re-chromatin immunoprecipitation experiments in which soluble chromatin immunoprecipitated with anti-V5 was re-immunoprecipitated with anti-HDAC2. IgG control refers to re-chromatin immunoprecipitation with anti-HDAC2.

vector encoding *CBX7* and with a reporter vector carrying the luciferase gene under the control of the *E-cadherin* promoter. As shown in Fig. 4*A* (*top*), CBX7 increases the transcriptional activity of the *E-cadherin* promoter in a dose-dependent manner. The same results were obtained on the NPA and TPC1 cell lines (Supplementary Fig. S2*A*). The treatment of cells with trichostatin A, a potent inhibitor of HDAC activity (31), cooperates with CBX7 to induce *E-cadherin* gene transcription (Fig. 4*A, bottom*). These results strongly suggest that CBX7 protein is involved in the *E-cadherin* gene transcription likely counteracting with the already known inhibitory effect of HDAC2 on this gene promoter.

To identify the region of CBX7 required for *E-cadherin* promoter activation, we constructed two CBX7 deletion mutants in the expression vector pCefl-HA: pCefl-HA-CBX7-CHROMO (1-100 amino acids) and pCefl-HA-CBX7-NOCHROMO (55-251 amino

acids). Transfection of the mutant pCefl-HA-CBX7-CHROMO, containing only the chromodomain, did not induce transcriptional activation of the *E-cadherin* promoter. Conversely, the mutant lacking the chromodomain, pCefl-HA-CBX7-NOCHROMO, induced a moderate activation of the *E-cadherin* promoter. Thus, these data indicate that chromodomain is not essential for the CBX7 transcriptional activity on the *E-cadherin* promoter (Fig. 4*B*).

Moreover, to show that the expression of E-cadherin is directly regulated by CBX7, we generated some clones of NPA cells (NPA 4-11 and NPA 5-11) in which *CBX7* cDNA was under the control of a tetracycline-regulated promoter. Western blot analysis (Fig. 4*C, top*) and quantitative RT-PCR experiment (Fig. 4*C, bottom*) show that the expression of CBX7 increases the levels of E-cadherin only after treatment with tetracycline.

To further confirm the role of CBX7 in the modulation of the *E-cadherin* gene, we evaluated the expression of the *E-cadherin* gene in the normal rat thyroid cell line PC Cl3 in which the synthesis of Cbx7 was suppressed by RNA interference. The knockdown of the *Cbx7* mRNA levels, observed at 48 h after treatment, resulted in the reduction of *E-cadherin* mRNA levels in comparison with the untreated cells or those treated with the nonsilencing control small interfering RNA (Fig. 4D).

To identify the regulatory elements essential for the activity of CBX7 on the *E-cadherin* promoter, we also tested some deletion mutants of the *E-cadherin* promoter: E-cadherin 601 and E-cadherin 211 (20, 21). Activation of *E-cadherin* promoter by CBX7 protein was maintained on full-length and −601 mutants of *E-cadherin* promoter. Conversely, the −211 mutant, which lacks a portion of −70/+54 sequence (able to bind CBX7), was not activated by CBX7 protein (Supplementary Fig. S2B).

CBX7 expression results in increased histone acetylation of the *E-cadherin* promoter. During the last years, chromatin remodeling and histone modifications have emerged as the main mechanisms in the control of gene expression and the connection between DNA methylation and histone deacetylation in the silencing of genes has been established (32–37).

Because we have shown previously that CBX7 (*a*) interacts with HDAC2 on the human *E-cadherin* promoter, (*b*) increases the transcriptional activity of the *E-cadherin* promoter in a dose-dependent manner, and (*c*) reduces the activity of HDACs, we hypothesized that the positive effect on *E-cadherin* activation by CBX7 may be due to its ability to reduce the HDAC activity on the *E-cadherin* promoter. Therefore, we have evaluated the lysine acetylation of histone tails at the *E-cadherin* promoter.

HEK 293 cells were transiently transfected with V5-tagged CBX7 expression vector or empty vector. Then, the cells were crosslinked and DNA-chromatin was immunoprecipitated with anti-H3 or anti-H4 acetylated or IgG antibodies. The immunoprecipitated chromatin was subsequently analyzed by quantitative PCR using primers spanning the region of the *E-cadherin* promoter

Figure 4. CBX7 enhances *E-cadherin* promoter activity. *A, top,* dose-response analysis of increasing amounts of *CBX7* on the *E-cadherin* luciferase-reporter vector transiently transfected into HEK 293 cells. Western blot analysis confirmed the increasing amounts of CBX7 expression. α-Tubulin expression served as a control of equal protein loading. *Bottom,* dose-response analysis of increasing amounts of *CBX7* on the *E-cadherin* luciferase-reporter vector transiently transfected into HEK 293 cells treated or not with 300 nmol/L of HDAC inhibitor trichostatin A (*TSA*). *B,* dose-response analysis of increasing amounts of *CBX7* and the two *CBX7*-deletion mutants (schematically illustrated in Fig. 1*B*) on the *E-cadherin* luciferase-reporter vector transiently transfected into HEK 293 cells. *C, top,* Western blot analysis of CBX7 and E-cadherin expression in the NPA cell clones 4-11 and 5-11 treated or not with tetracycline. The treatment with tetracycline (+*tet*) was indicated on the top. α-Tubulin expression served as a control of equal protein loading. *Bottom,* quantitative RT-PCR (*qRT-PCR*) analysis of E-cadherin expression in the same NPA cell clones. The relative expression indicates the relative change in E-cadherin expression levels between treated cells versus the untreated ones, assuming that the value of E-cadherin expression in the untreated cells is equal to 1. *D, Cbx7* and *E-cadherin* gene expression was evaluated by RT-PCR in rat PC Cl3 cells after treatment with small interfering RNA against rat *Cbx7*. The expression of *GAPDH* was used to normalize the amounts of RNAs used in the experiment.
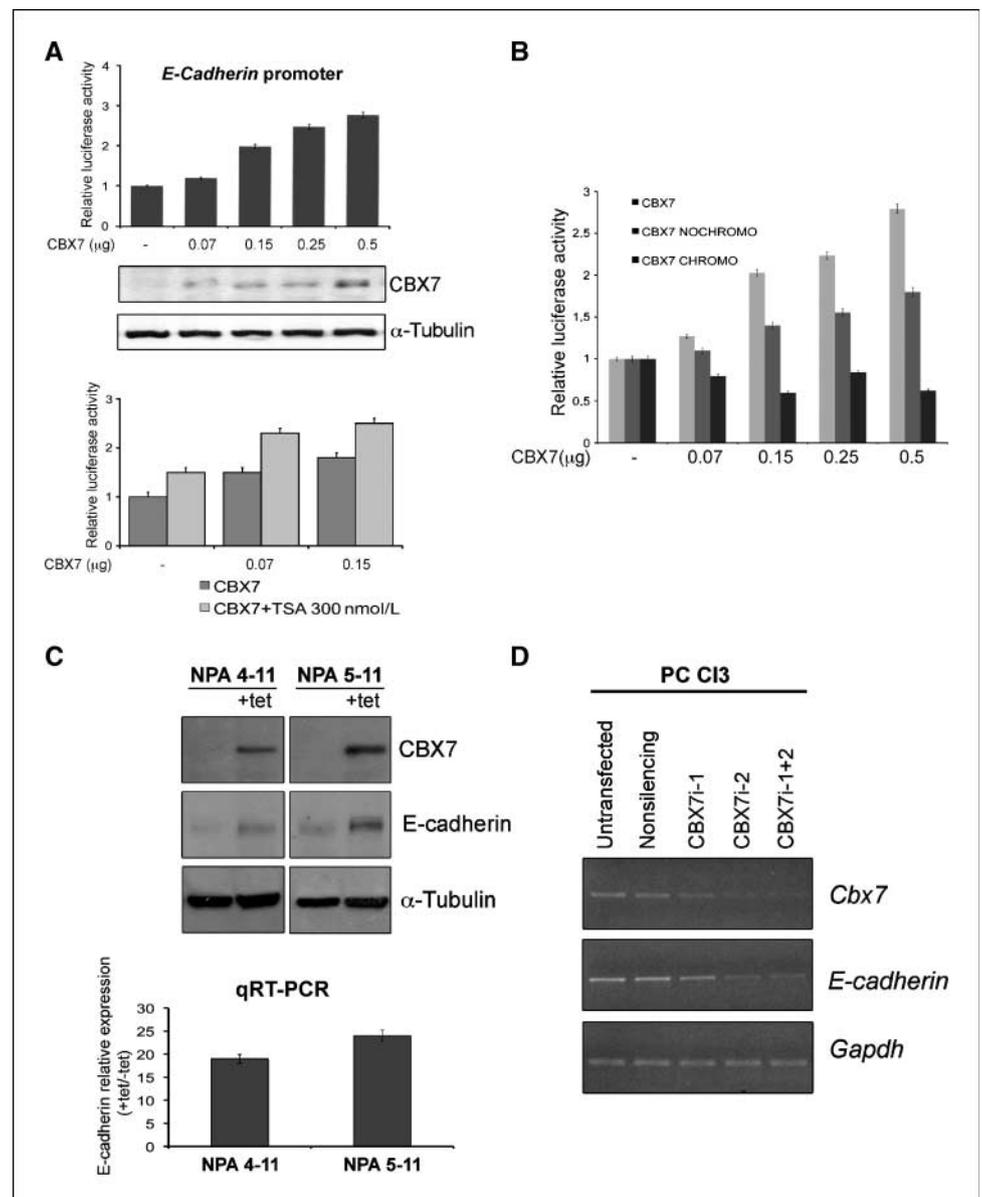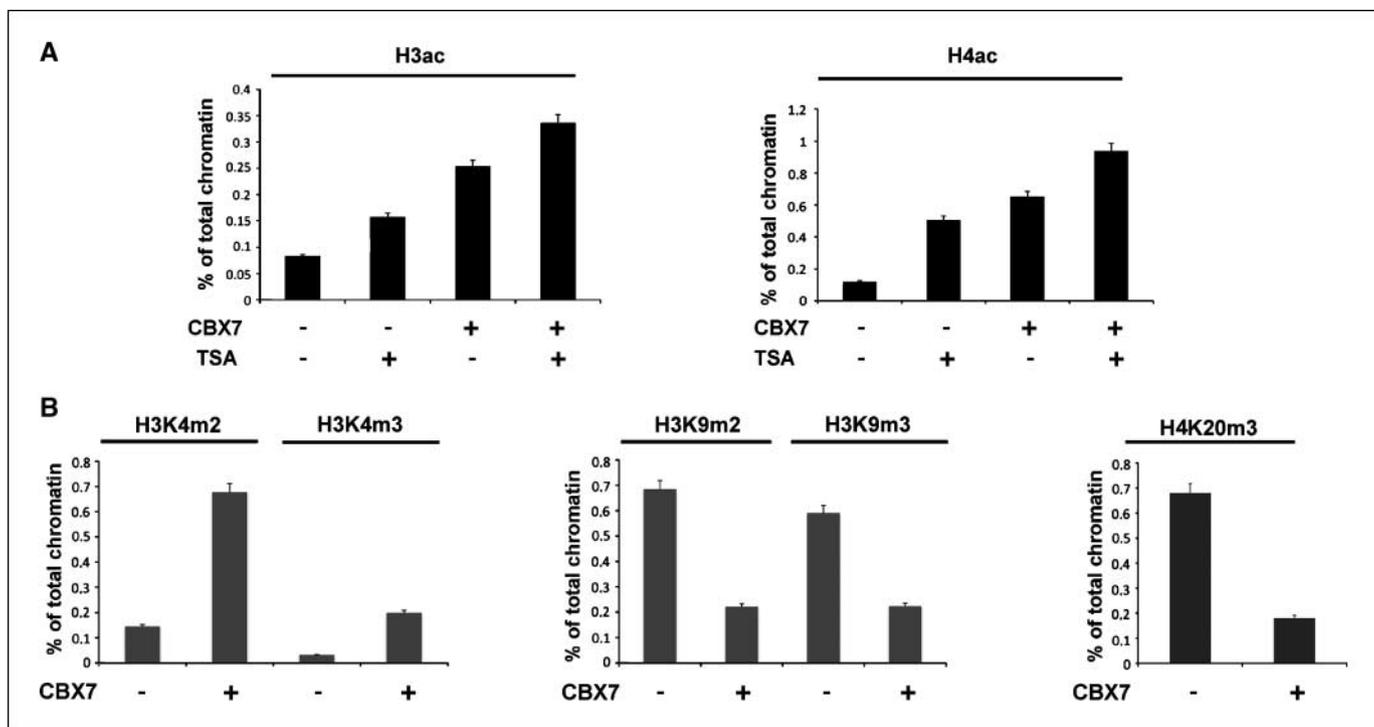
Figure 5. Analysis of the histone code modifications of the human *E-cadherin* promoter. *A,* HEK 293 cells transiently transfected with V5-tagged CBX7 expression or empty vectors, and treated or not with trichostatin A for 24 h, were subjected to chromatin immunoprecipitation using anti-acetyl histone H3 (*H3ac; left*) and anti-acetyl histone H4 (*H4ac; right*) and analyzed by quantitative RT-PCR for the *E-cadherin* promoter. *B,* HEK 293 cells transiently transfected with V5-tagged CBX7 expression or empty vectors were subjected to chromatin immunoprecipitation using anti-H3K4m2 and anti-H3K4m3 (*left*), anti-H3K9m2 and anti-H3K9m3 (*middle*), and anti-H4K20m3 (*right*) and analyzed by quantitative RT-PCR for the *E-cadherin* promoter.

(-70 bp upstream to $+54$ bp downstream to the TSS; ref. 38). As shown in Fig. 5A, higher amounts of H3 and H4 acetylated tails were detected in the *E-cadherin* promoter in the cells transfected with CBX7, with respect to those detected in mock-transfected cells, indicating an increased histone acetylation in CBX7-transfected cells, likely due to the ability of CBX7 to reduce HDAC activity. We also treated the cells, transfected or not with CBX7, with trichostatin A to verify the HDAC activity on H3 and H4 tails. As shown in the same figure, there were higher amounts of H3 and H4 acetylated tails in CBX7-transfected samples treated with trichostatin A than in untreated cells. These results indicate that CBX7 protein regulates the E-cadherin expression by modifying histone acetylation at its promoter, likely reducing HDAC activity.

Increased methylation of H3K4 and decreased methylation of H3K9 and H4K20 in CBX7-transfected cells. Lysine methylation can have different effects depending on which residue is modified: methylation of H3K4 and H3K36 is generally associated with transcribed chromatin; in contrast, methylation of H3K9, H3K27, and H4K20 generally correlates with gene repression (38). Therefore, we have evaluated the lysine methylation status of histone tails of *E-cadherin* promoter in presence or absence of CBX7.

HEK 293 cells were transiently transfected with V5-tagged CBX7 or empty vectors and crosslinked, and DNA-chromatin was immunoprecipitated with anti-H3K4m2, anti-H3K4m3, anti-H3K9m2, anti-H3K9m3, and anti-H4K20m3 or IgG antibodies. The immunoprecipitated chromatin was subjected to PCR with specific primers for the *E-cadherin* promoter region ($-70/+54$).

Higher amounts of chromatin immunoprecipitated for H3K4m2 and H3K4m3 were observed in the CBX7-transfected cells

compared with the control ones, indicating that this lysine is methylated in a higher proportion in CBX7-transfected cells with respect to that observed in control cells. Conversely, in the case of chromatin immunoprecipitated for the H3K9m2, H3K9m3, and H4K20m3, higher amounts of chromatin were detected in control cells, indicating that these sites were methylated at a higher level in the control cells versus CBX7-transfected cells (Fig. 5B). These data indicate that CBX7 is able to alter the methylation status of specific lysines of *E-cadherin* promoter, promoting the transcriptional activity of *E-cadherin* promoter.

CBX7 and E-cadherin expression levels are correlated in human thyroid carcinomas. E-cadherin down-regulation, due to epigenetic mechanisms, including transcriptional repression, also mediated by HDAC activity, and promoter hypermethylation is a frequent event during human cancer progression (39, 40). Because previous experiments showed that CBX7 expression was lost in most advanced thyroid cancers, we hypothesized the down-regulation of E-cadherin as a possible mechanism by which loss of CBX7 is involved in advanced stages of thyroid carcinogenesis. This hypothesis was also supported by recent results showing a role of polycomb repressive complex 1/2 in the regulation of E-cadherin expression (41).

Therefore, we analyzed *CBX7* and *E-cadherin* mRNA levels in human thyroid carcinomas of different histotypes (Fig. 6A). *CBX7* and *E-cadherin* mRNA levels were drastically reduced in anaplastic thyroid carcinoma, whereas just a weak decrease was observed for both genes in papillary thyroid carcinoma. The epithelial-to-mesenchymal transition in our tumor samples was also confirmed by the increased N-cadherin expression (Fig. 6A).

We found a positive statistical correlation between CBX7 and E-cadherin expression in human thyroid carcinomas as shown in Fig. 6B. We also compared CBX7 and E-cadherin at protein level, by immunohistochemical analysis, confirming that E-cadherin protein expression parallels that of CBX7 (Fig. 6C).

Because hypermethylation of the *E-cadherin* promoter has been postulated to play a critical role in the loss of E-cadherin expression and has been reported previously in other cancers, we decided to investigate the DNA methylation status of *E-cadherin* promoter (42). We analyzed DNA methylation status of 26 CpG sites located in a 368-bp region spanning the *E-cadherin* gene TSS (Fig. 6D, inset) on 16 papillary thyroid carcinomas, 15 follicular variants of papillary thyroid carcinomas, 4 anaplastic thyroid carcinomas, and 4 normal thyroid tissue samples. A very low level of methylation was present in both normal and tumor samples, with the exception of only one anaplastic thyroid carcinoma sample in which a high degree of methylation was detected (Fig. 6D).

Therefore, epigenetic mechanisms, other than hypermethylation of the *E-cadherin* promoter, have a critical role in the down-regulation of E-cadherin expression.
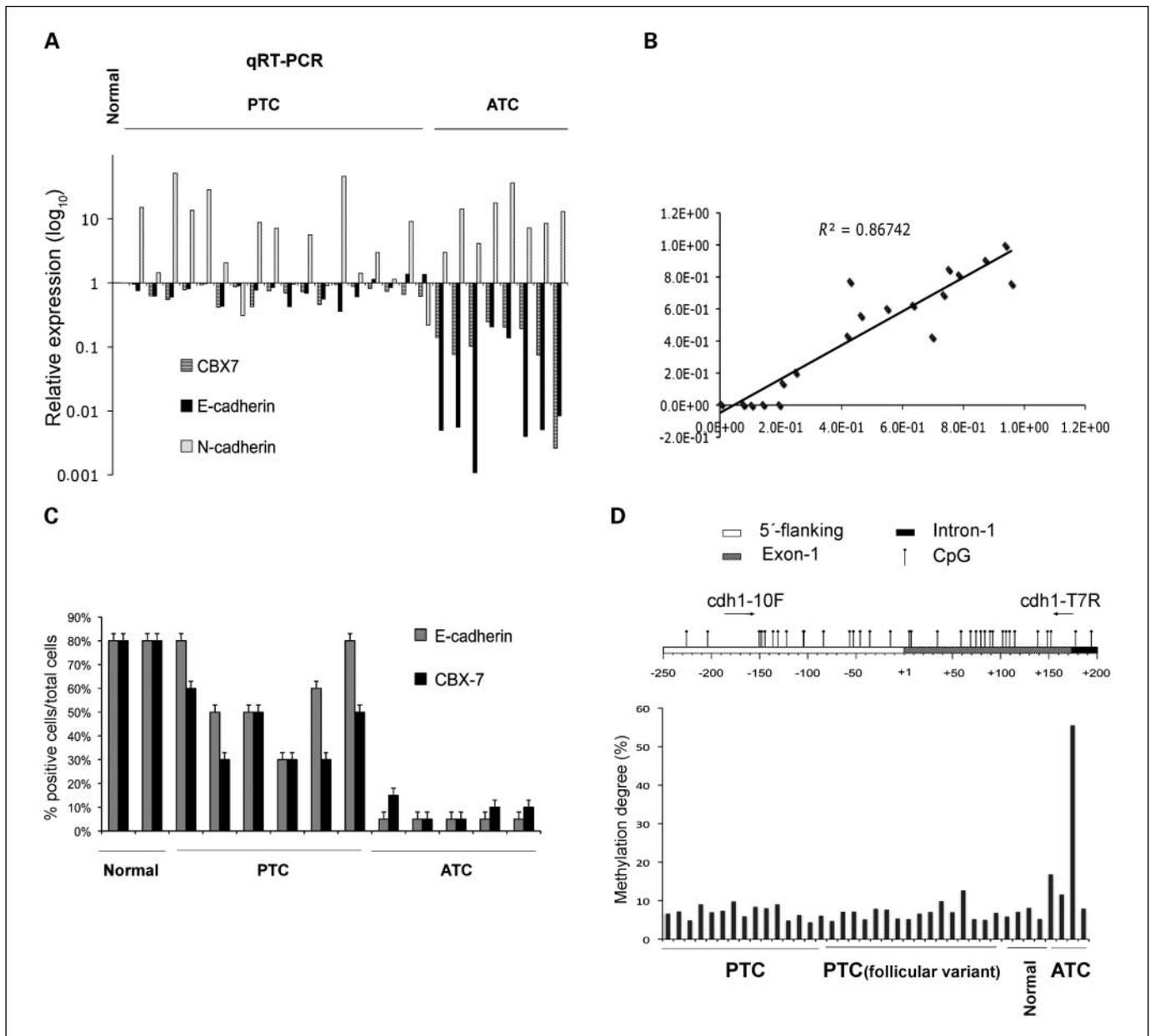

Figure 6. *CBX7* and *E-cadherin* gene expression levels are correlated in human thyroid carcinomas. *A*, CBX7, *E-cadherin*, and *N-cadherin* gene expression in thyroid tumor samples was analyzed by quantitative RT-PCR. Relative expression indicates the change in expression levels between tumor and normal samples, assuming that the value of each normal sample is equal to 1. *B*, positive statistical correlation between CBX7 and E-cadherin expression in human thyroid carcinomas analyzed in *A*. R^2, Pearson correlation coefficient. *C*, immunohistochemical analysis of normal and tumor samples stained with anti-CBX7 and anti-E-cadherin antibodies. The percentage of positive cells for the staining/total number of cells was reported. *D, top,* positions of the primers used for amplifications of the region spanning from nucleotide −200 to + 200 of *E-cadherin* with respect to the TSS; *bottom,* average methylation degree of 26 CpG sites at *E-cadherin* promoter in human thyroid carcinomas. *PTC,* papillary thyroid carcinoma; *ATC,* anaplastic thyroid carcinoma.

Cancer Research

Discussion

Our group has reported previously that *CBX7* gene is drastically down-regulated in thyroid carcinomas and its expression progressively decreases with malignant grade and neoplastic stage (8). These data suggest that the loss of CBX7 expression may be strictly correlated with the acquisition of invasiveness accompanied by the loss of the epithelial features and the gain of a mesenchymal phenotype, a process known as epithelial-to-mesenchymal transition. E-cadherin is a main component of the cell-cell adhesion junctions that plays a principal role in maintaining normal epithelial cell morphology, therefore emerging as one of the caretakers of the epithelial phenotype. In most cancers, E-cadherin down-regulation during neoplastic progression occurs by epigenetic mechanisms, including transcriptional repression, in some cases mediated by HDAC activity (40), and hypermethylation of the promoter (42). Only in a few cases mutations have been found in the *E-cadherin* gene leading to the absence or the expression of a nonfunctional protein (29). For this reason, we evaluated E-cadherin expression in human thyroid carcinomas of different histotypes: an evident correlation was found between CBX7 and E-cadherin expression levels in human thyroid carcinomas, both being drastically down-regulated in anaplastic thyroid carcinomas in comparison with the normal thyroid tissue. Interestingly, no hypermethylation of *E-cadherin* promoter was observed in thyroid carcinomas. Therefore, we have hypothesized a role for CBX7 as a transcriptional repressor of E-cadherin. We have shown that CBX7 binds to *E-cadherin* gene promoter *in vitro* by electrophoretic mobility shift assay and *in vivo* by chromatin immunoprecipitation and is able to positively regulate the activity of *E-cadherin* promoter. At the same time, a proteomic approach, aimed to unravel the mechanism by which the loss of CBX7 expression is involved in cancer progression, has identified HDAC2 among the CBX7 interacting proteins. HDACs regulate the expression and activity of numerous proteins involved in both cancer initiation and cancer progression, inducing a nonpermissive chromatin conformation that prevents the transcription of genes encoding proteins involved in tumorigenesis. HDACs are often overexpressed in many tumors (25).

Here, we show that CBX7 physically interacts with HDAC2 protein inhibiting its activity. Chromatin immunoprecipitation shows that both HDAC2 and CBX7 bind the *E-cadherin* promoter. We also show the ability of CBX7 to positively regulate E-cadherin expression by interacting with HDAC2 and inhibiting its activity on the *E-cadherin* promoter. Further, we show that, in the presence of the CBX7 protein, there is an increased histone acetylation of the *E-cadherin* promoter, validating our hypothesis that CBX7 recruits HDCA2 on the *E-cadherin* promoter. Moreover, we showed modifications in the histone methylation state on the *E-cadherin* promoter in the cells transfected with CBX7 confirming a relationship between acetylation and DNA methylation (36).

It is noteworthy that, among CBX7 interacting proteins, we have also identified an arginine methylation protein that can have a regulator effect on HDACs activity, because a cross-talk between histone acetylation and arginine methylation has also been observed (43). In fact, histone deacetylation is a prerequisite for PRMT5-mediated H3 and H4 arginine methylation, whereas histone acetylation enhances H3R17 methylation by PRMT4 (44–46).

In conclusion, here we propose a novel pathway regulating the progression step of carcinogenesis in which the CBX7 protein, the loss of expression of which correlates with a highly malignant phenotype, is a key molecule. Indeed, our results indicate that the loss of CBX7 expression contributes to cancer progression by down-regulating E-cadherin expression because of the lack of its inhibitory effect on HDAC activity on the *E-cadherin* promoter.

Disclosure of Potential Conflicts of Interest

No potential conflicts of interest were disclosed.

References

1. Gil J, Bernard D, Martinez D, Beach D. Polycomb CBX7 has a unifying role in cellular lifespan. Nat Cell Biol 2004; 6:67–72.
2. Bernard D, Martinez-Leal JF, Rizzo S, et al. CBX7 controls the growth of normal and tumor-derived prostate cells by repressing the *Ink4a/Arf* locus. Oncogene 2005;24:5543–51.
3. Scott CL, Gil J, Hernando E, et al. Role of the chromobox protein CBX7 in lymphomagenesis. Proc Natl Acad Sci U S A 2007;104:5389–94.
4. Schuettengruber B, Chourrout D, Vervoort M, Leblanc B, Cavalli G. Genome regulation by polycomb and trithorax proteins. Cell 2007;128:735–45.
5. Wu JI, Lessard J, Crabtree GR. Understanding the words of chromatin regulation. Cell 2009;136:200–6.
6. Bernstein E, Duncan EM, Masui O, Gil J, Heard E, Allis CD. Mouse polycomb proteins bind differentially to methylated histone H3 and RNA and are enriched in facultative heterochromatin. Mol Cell Biol 2006;26:2560–9.
7. Lund AH, van Lohuizen M. Polycomb complexes and silencing mechanisms. Curr Opin Cell Biol 2004; 16:239–46.
8. Pallante P, Federico A, Berlingieri MT, et al. Loss of the CBX7 gene expression correlates with a highly malignant phenotype in thyroid cancer. Cancer Res 2008;68: 6770–8.
9. Hedinger C, Williams ED, Sobin LH. The WHO histological classification of thyroid tumours: a commentary on the second edition. Cancer 1989;63:908–11.
10. Kondo T, Ezzat S, Asa SL. Pathogenetic mechanisms in thyroid follicular-cell neoplasia. Nat Rev Cancer 2006; 6:292–306.
11. Pallante P, Berlingieri MT, Troncone G, et al. UbcH10 overexpression may represent a marker of anaplastic thyroid carcinomas. Br J Cancer 2005;93:464–71.
12. Fusco A, Berlingieri M, Di Fiore PP, Portella G, Grieco M, Vecchio G. One- and two-step transformations of rat thyroid epithelial cells by retroviral oncogenes. Mol Cell Biol 1987;7:3365–70.
13. Fedele M, Visone R, De Martino I, et al. HMGA2 induces pituitary tumorigenesis by enhancing E2F1 activity. Cancer Cell 2006;9:459–71.
14. Pierantoni GM, Esposito F, Giraud S, Bienvenut WV, Diaz JJ, Fusco A. Identification of new high mobility group A1 associated proteins. Proteomics 2007;7:3735–42.
15. Fedele M, Fidanza V, Battista S, et al. Haploinsufficiency of the *Hmga1* gene causes cardiac hypertrophy and myelo-lymphoproliferative disorders in mice. Cancer Res 2006;66:2536–43.
16. Livak KJ, Schmittgen T. Analysis of relative gene expression data using real-time quantitative PCR and the $2(-\Delta\Delta C(T))$. Method Methods 2001;25:402–8.
17. Frank SR, Schroeder M, Fernandez P, Taubert S, Amati B. Binding of c-Myc to chromatin mediates mitogen-induced acetylation of histone H4 and gene activation. Genes Dev 2001;15:2069–82.
18. Dignam JD, Lebovitz RM, Roeder RG. Accurate transcription initiation by RNA polymerase II in a soluble extract from isolated mammalian nuclei. Nucleic Acids Res 1983;11:1475–89.
19. Pierantoni GM, Rinaldo C, Esposito F, Mottolese M, Soddu S, Fusco A. High mobility group A1 (HMGA1) proteins interact with p53 and inhibit its apoptotic activity. Cell Death Differ 2006;13:1554–63.
20. Ji X, Woodard AS, Rimm DL, Fearon ER. Transcriptional defects underlie loss of E-cadherin expression in breast cancer. Cell Growth Differ 1997;8:773–8.
21. Hajra KM, Ji X, Fearon ER. Extinction of E-cadherin expression in breast cancer via a dominant repression pathway acting on proximal promoter elements. Oncogene 1999;51:7274–9.
22. Li LC, Dahiya R. MethPrimer: designing primers for methylation PCRs. Bioinformatics 2002;18:1427–31.
23. Ehrich M, Nelson M, Stanssens P, et al. Quantitative high-throughput analysis of DNA methylation patterns

by base-specific cleavage and mass spectrometry. Proc Natl Acad Sci U S A 2005;102:15785–90.

24. Shevchenko A, Keller P, Scheiffele P, Mann M, Simons K. Identification of components of trans-Golgi network-derived transport vesicles and detergent-insoluble complexes by nanoelectrospray tandem mass spectrometry. Electrophoresis 1997;18:2591–600.

25. Glozak MA, Seto E. Histone deacetylases and cancer. Oncogene 2007;26:5420–32.

26. Kruh J. Effects of sodium butyrate, a new pharmacological agent, on cells in culture. Mol Cell Biochem 1982;42:65–82.

27. Rada-Iglesias A, Enroth S, Ameur A, et al. Butyrate mediates decrease of histone acetylation centered on transcription start sites and down-regulation of associated genes. Genome Res 2007;17:708–19.

28. Peinado H, Ballestar E, Esteller M, Cano A. Snail mediates E-cadherin repression by the recruitment of the Sin3A/histone deacetylase 1 (HDAC1)/HDAC2 complex. Mol Cell Biol 2004;24:306–19.

29. Thiery JP. Epithelial-mesenchymal transitions in tumour progression. Nat Rev Cancer 2002;2:442–54.

30. Thiery JP, Sleeman J. Complex networks orchestrate epithelial-mesenchymal transitions. Nat Rev Mol Cell Biol 2006;7:131–42.

31. Ou JN, Torrisani J, Unterberger A, et al. Histone deacetylase inhibitor trichostatin A induces global and gene-specific DNA demethylation in human cancer cell lines. Biochem Pharmacol 2007; 73:1297–307.

32. Marks P, Rifkind RA, Richon VM, et al. Histone deacetylases and cancer: causes and therapies. Nat Rev Cancer 2001;1:194–202.

33. Bolden JE, Peart M, Johnstone RW. Anticancer activities of histone deacetylase inhibitors. Nat Rev Drug Discov 2006;5:769–84.

34. Minucci S, Pelicci PG. Histone deacetylase inhibitors and the promise of epigenetic (and more) treatments for cancer. Nat Rev Cancer 2006;6:38–51.

35. Smith CL. A shifting paradigm: histone deacetylases and transcriptional activation. Bioessays 2008;30:15–24.

36. Kouzarides T. Chromatin modifications and their function. Cell 2007;128:693–705.

37. van Leeuwen F, van Steensel B. Histone modifications: from genome-wide maps to functional insights. Genome Biol 2005;6:113.

38. Li B, Gogol M, Carey M, Lee D, Seidel C, Workman JL. The role of chromatin during transcription. Science 2007;316:1050–4.

39. Koizume S, Tachibana K, Sekiya T, Hirohashi S, Shiraishi M. Heterogeneity in the modification and involvement of chromatin components of the CpG island of the silenced human *CDH1* gene in cancer cells. Nucleic Acids Res 2002;30:4770–80.

40. Peinado H, Portillo F, Cano A. Transcriptional regulation of cadherins during development and carcinogenesis. Int J Dev Biol 2004;48:365–75.

41. Cao Q, Yu J, Dhanasekaran SM, et al. Repression of E-cadherin by the polycomb group protein EZH2 in cancer. Oncogene 2008;27:7274–84.

42. Hajra KM, Fearon E. Cadherin and catenin alterations in human cancer. Genes Chromosomes Cancer 2002;34:255–68.

43. Huang S, Litt M, Felsenfeld G. Methylation of histone H4 by arginine methyltransferase PRMT1 is essential *in vivo* for many subsequent histone modifications. Genes Dev 2005;19:1885–93.

44. Pal S, Vishwanath S, Erdjument-Bromage H, Tempst P, Sif S. Human SWI/SNF-associated PRMT5 methylates histone H3 arginine 8 and negatively regulates expression of ST7 and NM23 tumor suppressor genes. Mol Cell Biol 2004;24:9630–45.

45. Pal S, Yun R, Datta A, et al. mSin3A/histone deacetylase 2- and PRMT5-containing Brg1 complex is involved in transcriptional repression of the Myc target gene cad. Mol Cell Biol 2003;23: 7475–87.

46. Kirmizis A, Santos-Rosa H, Penkett CJ, et al. Arginine methylation at histone H3R2 controls deposition of H3K4 trimethylation. Nature 2007;449: 928–32.

Cancer Research

Chromobox Protein Homologue 7 Protein, with Decreased Expression in Human Carcinomas, Positively Regulates E-Cadherin Expression by Interacting with the Histone Deacetylase 2 Protein

Antonella Federico, Pierlorenzo Pallante, Mimma Bianco, et al.

Updated version	Access the most recent version of this article at: doi:10.1158/0008-5472.CAN-09-1542
Supplementary Material	Access the most recent supplemental material at: http://cancerres.aacrjournals.org/content/suppl/2009/08/21/0008-5472.CAN-09-1542.DC1

Cited articles	This article cites 46 articles, 17 of which you can access for free at: http://cancerres.aacrjournals.org/content/69/17/7079.full.html#ref-list-1
Citing articles	This article has been cited by 6 HighWire-hosted articles. Access the articles at: /content/69/17/7079.full.html#related-urls

E-mail alerts	Sign up to receive free email-alerts related to this article or journal.
Reprints and Subscriptions	To order reprints of this article or to subscribe to the journal, contact the AACR Publications Department at pubs@aacr.org.
Permissions	To request permission to re-use all or part of this article, contact the AACR Publications Department at permissions@aacr.org.